Hypercrosslinked Polystyrene Microspheres with Bimodal Pore Size Distribution and Controllable Macroporosity

Qingquan Liu,[1,2] Li Wang,[1] Weiting Yu,[1] Anguo Xiao,[1] Haojie Yu,[1] Jia Huo[1]

[1]*State Key Laboratory of Chemical Engineering, College of Materials Science and Chemical Engineering, Zhejiang University, Hangzhou 310027, China*
[2]*College of Chemistry and Chemical Engineering, Hunan University of Science and Technology, Xiangtan 411201, China*

Received 9 February 2009; accepted 3 September 2009
DOI 10.1002/app.31422
Published online 20 November 2009 in Wiley InterScience (www.interscience.wiley.com).

ABSTRACT: A combination of suspension polymerization and postcrosslinking was used to prepare hypercrosslinked polystyrene (H-PS) microspheres with controllably bimodal pore size distribution in the presence of toluene and polypropylene (PP) as a coporogen. The proportion of PP in the coporogen was changed to investigate the influence of the coporogen composition on the pore structure of the H-PS microspheres. The addition of a small amount of PP achieved the aim of a clearly bimodal pore size distribution and the control of the macroporosity of the H-PS microspheres, which have potential application in the preparation of catalyst supports. The specific surface area of the H-PS microspheres could be adjusted in the range 380–790 m^2/g by changes in the concentration of PP in the coporogen. Moreover, the H-PS microspheres displayed all the characteristics of Davankov-type resins by their ability to be swollen in both thermodynamically poor solvents such as water and good solvents such as toluene. Finally, the possible mechanism of porosity formation during polymerization and postcrosslinking was also examined by a combination of pore structure data and the appearance of the microspheres before and after postcrosslinking. © 2009 Wiley Periodicals, Inc. J Appl Polym Sci 116: 84–92, 2010

Key words: crosslinking; polystyrene; macroporous polymers

INTRODUCTION

Hypercrosslinked polystyrene (H-PS) is a certain kind of material with a high specific surface area (SSA) and a strong adsorption ability and, thus, is widely used in many applications, such as liquid chromatograpgy,[1,2] membrane materials for separation,[3] biomedicine,[4] and catalyst supports.[5–7] Different porous materials are used in various applications because of their diverse pore morphologies.[8,9] In the application of catalyst supports, for example, it was reported that materials with bimodal pore size distributions are better than those with unimodal distributions.[6] Davankov et al.[5] reported that H-PS-supported Pt nanoparticles with a mean diameter of about 2 nm exhibited good reaction selectivity during the oxidation of L-sorbose to 2-keto-L-gulonic acid, a vitamin C precursor. However, the microporous structure (<2.0 nm) of H-PS limited the reactant transport inside the metalated H-PS support and, consequently, the catalytic activity. Recently, they used H-PS materials with both micropores and macropores as a support to prepare identical metal/polymer nanocomposites. They found that the catalytic activity of the same oxidation reaction had a 4.6-fold increase compared with the former system.[7] Undoubtedly, this substantial increase in the catalytic activity was due to the presence of macropores, which facilitated L-sorbose transport and, consequently, the accessibility of the nanoparticle surface for reactants.

H-PS materials were introduced by Davankov and coworkers[10–12] in the 1970s. H-PS materials were prepared by the crosslinking of linear polystyrene in solution or slightly crosslinked styrene–divinylbenzene (DVB) copolymers in a highly swollen state in the presence of a Lewis acid as a catalyst, with the result that the H-PS materials were highly crosslinked, microporous, and unimodal. Recently, porous poly(divinylbenzene-*co*-vinylbenzyl chloride) microspheres were used as a precursor to synthesize H-PS materials with a bimodal pore size distribution and a controllable microporosity.[13] However, in the application of catalyst supports, to improve the catalytic efficiency, it is necessary to controllably prepare H-PS materials with a high macroporosity.[7] Our former work demonstrated that when the content of polypropylene (PP) in a PP/toluene coporogen is adjusted, one can obtain poly(divinylbenzene) microspheres with a controllable macroporosity. It, therefore, seems plausible that the copolymerization of

Correspondence to: L. Wang (opl_wl@dial.zju.edu.cn).

DVB with vinylbenzyl chloride (VBC) with PP and toluene as coporogens could produce H-PS materials with a bimodal pore size distribution and a controllable macroporosity.

In this study, we prepared porous precursor microspheres by the suspension polymerization of DVB and VBC in the presence of PP/toluene as a coporogen; then, the microspheres were further hypercrosslinked with the Lewis acid $FeCl_3$ as a catalyst. We investigated the effect of the PP content in the coporogen on the pore structure of the H-PS materials and propose a possible mechanism of pore formation.

EXPERIMENTAL

Materials

DVB (mixtures of isomers, 80% grade, Sigma-Aldrich Chemie, GmbH, Steinheim, Germany) was extracted with a 5% (w/w) hydroxyl sodium solution to remove the inhibitor and was then washed with deionized water until neutralization. After it was dried by anhydrous magnesium sulfate, it was distilled *in vacuo* and stored in the refrigerator. VBC (mixtures of isomers, 90% grade) was supplied by Acros Organics. PP [number-average molecular weight (M_n) = 3157, weight-average molecular weight = 13,417, polydispersity index = 4.25) was used as received. 2,2′-Azobisisobutyronitrile (AIBN) was purchased from Linfeng Chem Co., Ltd. (China). It was recrystallized from methanol and used as the initiator. Poly(vinyl alcohol) (PVA; weight-average molecular weight = 88,000), toluene, 1,2-dichloroethane (DCE), and $FeCl_3$ were also from Sinopharm Chemical Reagent Co., Ltd., and were used without further purification.

Preparation of the VBC–DVB precursor microspheres

VBC–DVB precursor microspheres were obtained via the conventional free-radical suspension polymerization in 100-cm^3 three-necked round-bottom flask reactors. A 60-cm^3 aqueous solution containing 0.3 g of PVA (0.5 wt %) and 1.98 g of NaCl (3.3 wt %) was charged into the glass reactor and then heated to 50°C under an argon atmosphere. At a stirring speed of 300 rpm, a mixture of 0.033 g of AIBN, 1.9 cm^3 of DVB, 1.7 cm^3 of VBC, and 2.4 cm^3 of porogen (toluene or PP in toluene) was added to the reactor. After the mixture was stirred under an argon atmosphere for 15 min, the mixture was heated to 80°C, and this process lasted for 6 h. After polymerization, the products were washed twice with hot water and three times with methanol and vacuum-filtered to remove the stabilizer, PVA. Finally, the products were dried in a vacuum oven at 50°C for at least 12 h.

Hypercrosslinking of the precursor microspheres

The precursor microspheres (1.5 g) were swollen in 40 cm^3 of DCE in 250-cm^3 three-necked round-bottom flask reactors overnight and then stirred under an argon atmosphere for 1 h before an additional 60 cm^3 of DCE containing 1.83 g of $FeCl_3$ was added. The mixture was continuously stirred for another 1 h to fully disperse the catalyst; it was then heated in an oil bath at 80°C for 8 h. After the completion of hypercrosslinking, the cooled products were dried by rotary evaporation to produce dark brown materials. Then, the H-PS materials were washed with methanol, HNO_3 in ethanol (pH = 1), and deionized water one by one; then they were dried in a vacuum oven at 50°C. Afterward, the H-PS materials were extracted with toluene at 160°C for 24 h in a Soxhlet extractor to remove the residual porogen and monomers and were then washed three times with methanol to ensure complete removal of the impurities. Finally, the products were dried in a vacuum oven at 50°C for no less than 12 h.

Characterization

Nitrogen sorption porosimetry was performed on a Micromeritics ASIC-2 (USA) under a liquid nitrogen temperature of 77.3 K after the samples were first heated in a tube *in vacuo* at 70°C for 12 h to remove the adsorbed materials from the surface. The data were manipulated by standard software to yield relevant porosity parameters, such as SSA, average pore size, and porosity. Because nitrogen sorption porosimetry may omit some data in the macroporous range, an Autopore IV 9500 was adopted as a complement. The surface morphology of the beads was determined by scanning electron microscopy (SEM; Hitachi, S4800). The solvent uptakes of the H-PS materials with toluene, methanol, and water were measured gravimetrically (g/g), with the dry polymer being weighed first and then the swollen one. The centrifuge method with a small glass sinter stick (2000 rpm, 20 min) was used to remove excess solvent.

RESULTS AND DISCUSSION

Preparation of the precursor and H-PS materials

PP, used as a porogen, has a low M_n (M_n = 3157) but a relatively high polydispersity index (4.25), which reveals that such PP has a broad molecular weight distribution and quite a great deal of PP has a considerably high molecular weight.

TABLE I
Characterization Data of the H-PS Materials

		HF01	HF02	HF03	HF04	HF05	HF06
PP in the coporogen (wt %)[a]		0	1	3	5	7	10
SSA (m^2/g; N_2 BET)		793.2	679.5	770.1	435.0	495.3	388.9
Pore area (m^2/g; Hg intrusion)		70.3	76.0	111.7	108.6	49.2	51.7
Pore volume (cm^3/g; N_2 sorption)		0.47	0.44	0.59	0.27	0.53	0.54
Average pore size (nm)	N_2 sorption	2.4	2.6	3.0	2.5	4.2	5.6
	Hg intrusion	11.1	11.7	12.7	10.7	34.5	51.4
Porosity (%)[b]	3–10 nm	2.19	2.85	3.81	4.46	1.60	1.56
	10–50 nm	4.32	5.59	9.12	6.81	2.99	1.98
	50–4000 nm	1.04	1.35	2.32	2.07	13.41	20.25

Reaction conditions of the suspension polymerization: DVB/coporogen = 1/1(v/v), DVB/VBC = 1/1(v/v), oil/water = 1/10 (v/v), reaction time = 6 h, and temperature = 80°C. Reaction conditions of postcrosslinking: catalyst = $FeCl_3$, reaction time = 8 h, and temperature = 80°C.

[a] Balance is toluene.

[b] Derived from Hg intrusion.

Therefore, in our study, we designed the experiment with the content of PP in the coporogen in the range 0–10 wt % in case a higher fraction of PP caused a high viscosity in the oil phase. Actually, in our experiment, with the content of PP no greater than 10%, the monomers (DVB and VBC) and coporogens (PP and toluene) generated a fairly homogeneous and transparent solution; this indicated a very good dispersion of PP in the monomer droplets. On the basis of this fact, a series of precursor and H-PS materials were prepared without any difficulty by changes in the content of PP in the coporogen (Table I). Possible reactions during suspension polymerization (step 1) and postcrosslinking (step 2) are presented in Figure 1.

Effect of the coporogen composition on SSA

In this article, SSA of the H-PS materials, derived from the Brunauer, Emmet, and Teller (BET)[14] method, and the total pore area, calculated by Hg intrusion, are presented in Table I and were used to investigate the effect of the coporogen on SSA. SSA of the precursor microspheres was too low to allow meaningful calculation and so were the other characterization data of the precursor microspheres. The

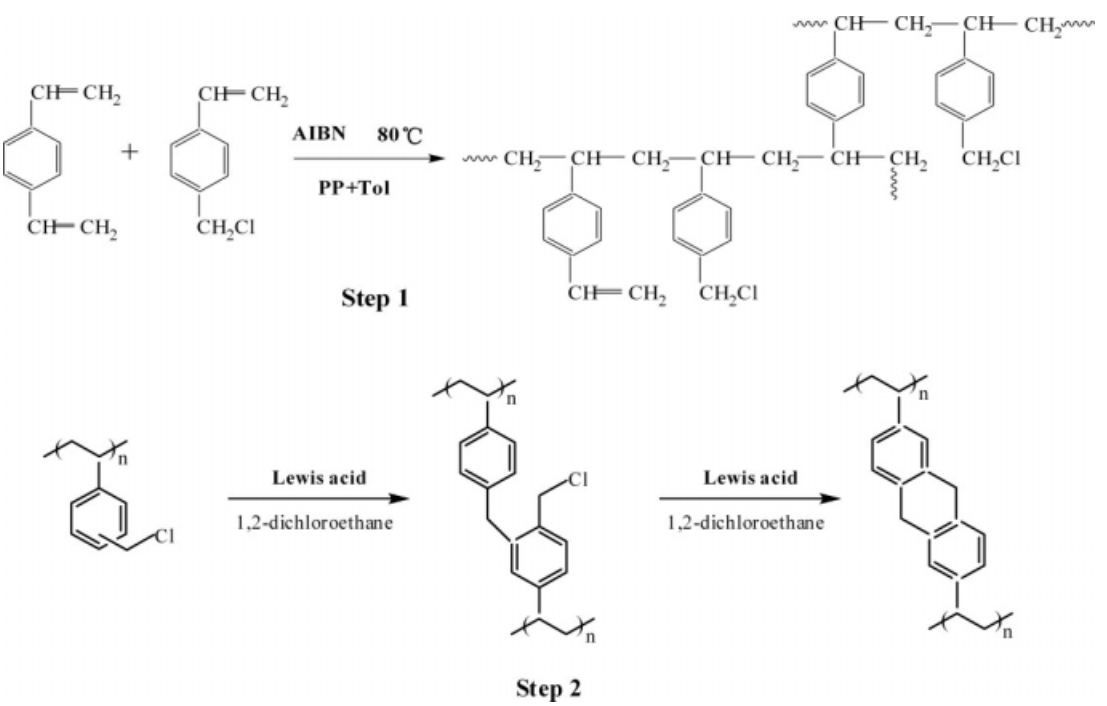

Figure 1 Possible reaction during suspension polymerization and postcrosslinking (Tol = toluene).

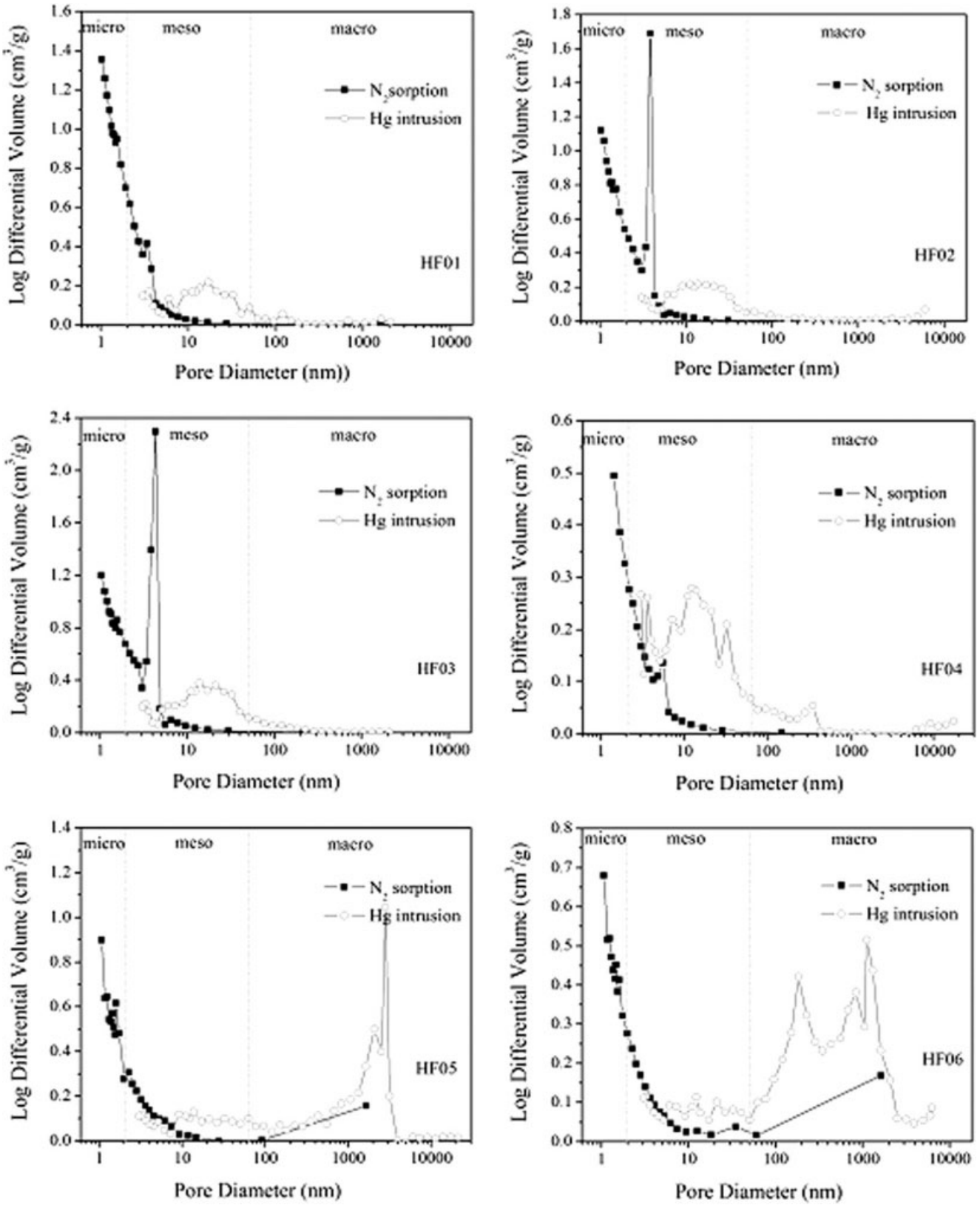

Figure 2 Pore size distribution curves derived from N_2 sorption and Hg intrusion for the H-PS materials.

reason for this phenomenon is discussed in the last part of the article. Therefore, only the data of the H-PS materials are presented in Table I.

Generally, the maximum value was achieved with toluene as the sole porogen [(HF01) where HF means the samples after hypercrosslinking and 01

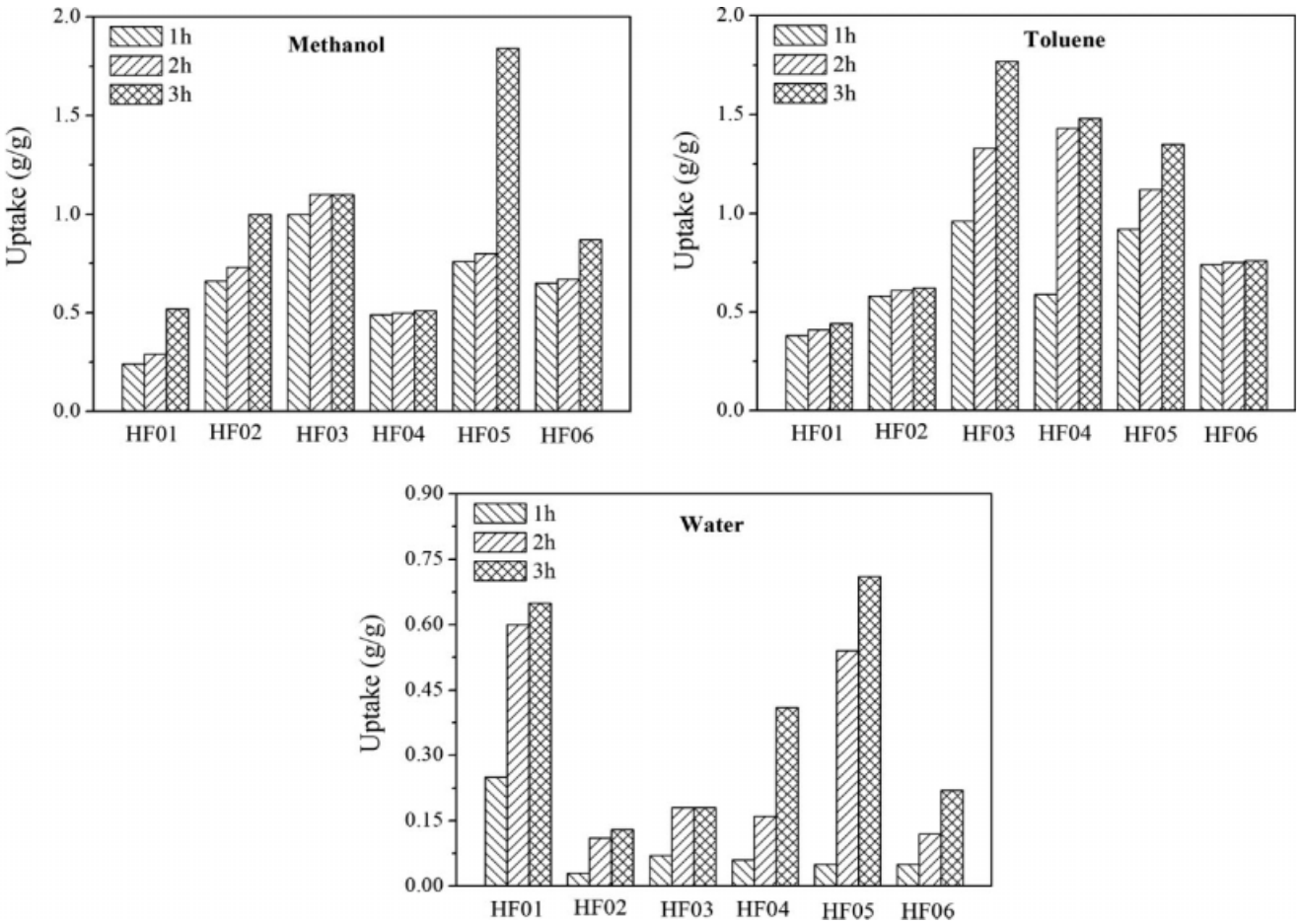

Figure 3 Solvent uptake data of the H-PS materials isolated at various times (hours) in different solvents.

means the sample number], which is easily understood according to the traditional phase separation. Later phase separation, induced by thermodynamically compatible solvents such as toluene, will lead to small pore diameters and high SSAs and vice versa.[15] Therefore, when the incompatible porogen PP was incorporated, SSA decreased at first. However, as the mass ratio of PP in the coporogen was increased, the values increased and subsequently fell, although there was a little scatter in the data. The previous tendency indicated that the addition of a low level of PP in the coporogen favored the improvement of SSA. This fact may have been due to the improved pore connectivity induced by some porous channels, which possibly formed during the extract process with benzene. Macintyre and Sherrington[16] also thought that low levels of an oligomeric porogen could improve the pore connectivity in the preparation of poly(divinylbenzene) microspheres. However, when the level of PP used continued to rise, the values underwent a fall because the presence of PP induced early phase separation, which favored the production of macropores and thus lowered the values.

At the same time, the values of total pore area obtained from Hg intrusion also reflected the pore structure of the H-PS materials to a certain extent. The values underwent a rise and a subsequent fall as the mass ratio of PP was increased. The maximum value was achieved by HF03, which further demonstrated the previous results from improved pore connectivity.

Effect of the coporogen composition on the average pore size and pore size distribution

The average pore sizes derived from N_2 sorption and Hg intrusion measurement are shown in Table I; to determine the average pore sizes of these products, we had to recognize the fact that the N_2 sorption experiment could not effectively probe pores with sizes greater than 200 nm, whereas the Autopore IV 9500 Hg intrusion instrument applied in our experiment likewise may not have accounted accurately for pores smaller than 3 nm. Therefore, it was meaningless to compare the data from these two methods.

Although there was some scatter in the data, overall, the average pore size increased as the amount of PP increased, which could be illustrated like just before: the presence of PP induced early phase separation, which contributed to the formation of macropores and resulted in a greater average pore size.

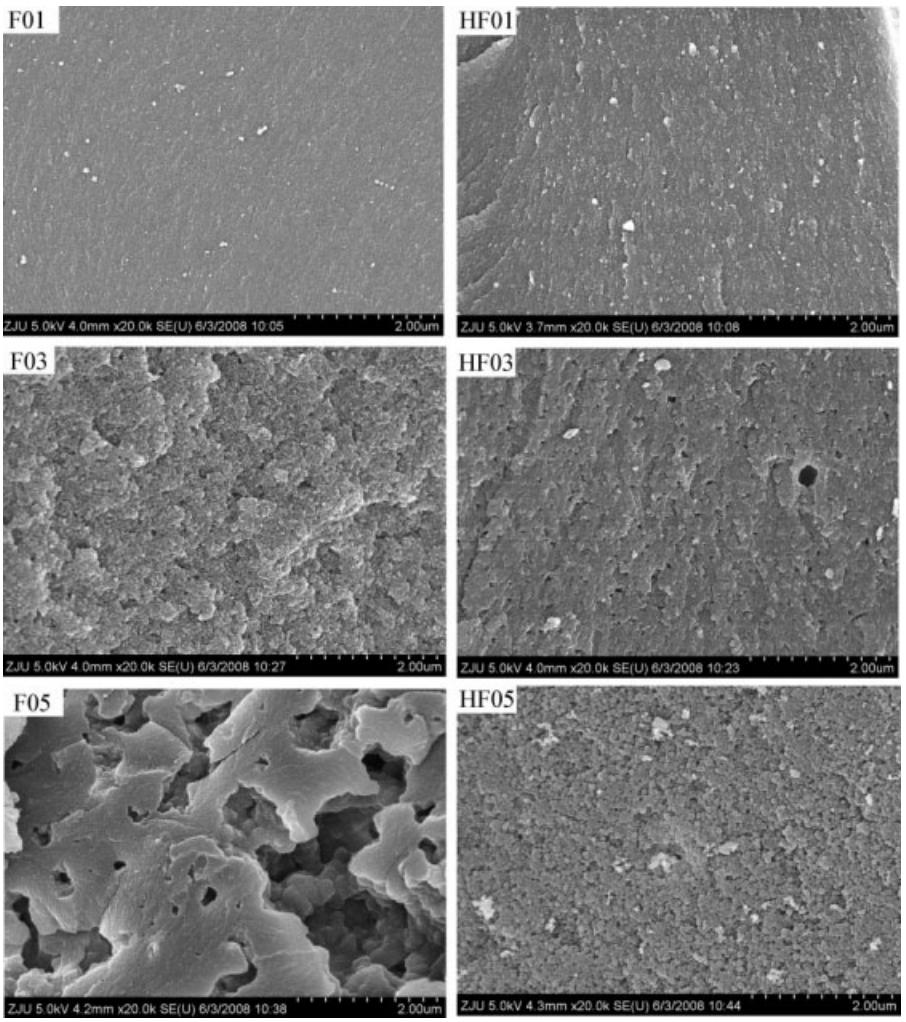

Figure 4 Internal morphology of the precursor and H-PS materials (F01, F03, F05, HF01, HF03, and HF05). F01 and HF01 are the samples before and after hypercrosslinking, respectively; so are F03 and HF03, F05 and HF05.

The pore size distribution provided a much better representation of the pore structure in the H-PS materials. Bearing in mind the experimental limitations on both the N_2 sorption derived parameters and that from the Hg intrusion experiments, we felt it necessary to combine these two sets of data together to get integrative distribution curves, such as those in Figure 2. From these curves, it was not hard to determine that some H-PS materials had clearly bimodal pore size distributions; those were HF01–HF04, with the pore size distribution mainly in the microporous range and mesoporous size, whereas HF05–HF06 had chiefly micropores and macropores. Such curves proved that we successfully synthesized H-PS with a clearly bimodal pore size distribution.

Effect of the coporogen composition on the porosity

Hg intrusion was used to obtain a percentage porosity in pore size ranges of 3–10, 10–50, and 50–4000 nm. These data are summarized and presented in Table I. The maximum mesoporosity of HF03 again indicated the improved pore connectivity by the low level of PP. Although there was a little scatter in the data, the macroporosity of the H-PS materials progressively increased with the mass ratio of PP porogen used, which indicated that the aim of a controllable macroporosity for the H-PS materials was achieved. Moreover, the values of the total pore volume derived from N_2 sorption were in agreement with the porosity obtained from Hg intrusion.

In addition, we also used the swollen measurement to characterize the porosity by measuring the mass of solvent absorbed by the H-PS materials. One of the most remarkable properties of H-PS materials is their response to solvents and, particularly, their tendency to adsorb highly polar solvents such as water. In our study, we studied not only the swell ratios of these H-PS materials in the thermodynamically compatible solvent toluene but also those in the thermodynamically poor solvents methanol and water. The solvent uptake data of these materials isolated at various times (hours) in different

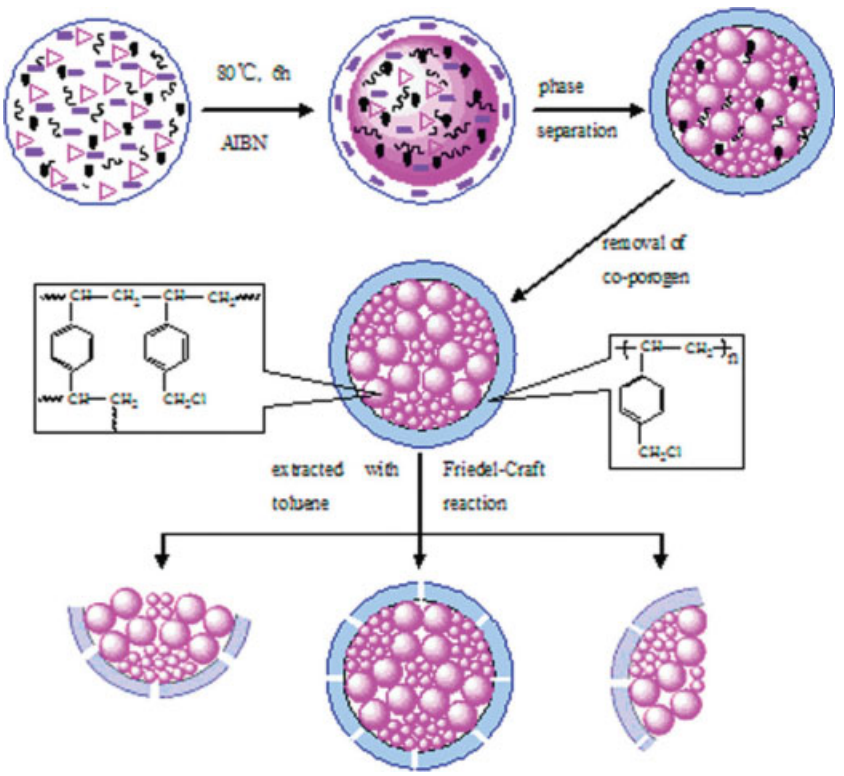

Figure 5 Schematic model of the possible pore formation mechanism: (●) toluene, (■) VBC, (▷) DVB, and (∿∿∿) PP. [Color figure can be viewed in the online issue, which is available at www.interscience.wiley.com.]

solvents are presented in Figure 3. The results indicated that the products could be swollen in both thermodynamically good and poor solvents. At the same time, these data were consistent with the known compatibility of polystyrene with the various solvents. The uptake was greater for toluene and lower for methanol and water.

SEM of the precursor and H-PS materials

The internal morphology of the H-PS materials before and after the hypercrosslinking reaction was observed under SEM with gold-coated samples. Some typical photographs are presented in Figure 4. The precursors were spheric, but samples HF01 ~ HF06 seldom retained sphericity. The reason is discussed later.

From these photos, on the one hand, we determined that in general, after hypercrosslinking reaction, the coarse surface morphology became smooth. We think this was because, in the second step of the reaction, that is, the process of the hypercrosslinking reaction, a lot of microporous structures were further formed, and that caused the smoothness in the surface morphology. On the other hand, with the level of PP used increasing, the surface became coarser and coarser. This phenomenon was due to the increase in the amount of PP used, which allowed the microgel particles to fuse, aggregate, and form larger particles during early phase separation.[15]

Possible pore formation mechanism

According to the mentioned facts, the characterization data of the pore structure of all the precursors were almost zero, and the H-PS materials could hardly retain a spherical shape. We propose the possible pore formation mechanism with the schematic model presented in Figure 5.

With all kinds of monomers, initiators, and porogens supplied, after the addition of heating, the consumption rate of DVB was absolutely faster than that of VBC because of the higher reactivity of the monomer DVB. Then, the early phase separation induced by the PP porogen took place, and a macroporous structure began to form, which was followed by the late phase separation caused by toluene and the formation of micropores. When all of the DVB was completely consumed, a small quantity of VBC was still unreacted. By this time, the residual VBC aggregated on the surface of the copolymer particles or between the voids formed by the copolymer particles. The less active VBC continued to polymerize, and the formed polymer covered outside the preformed copolymer particles. As a result, when suspension polymerization finished, the preformed copolymer aggregates were

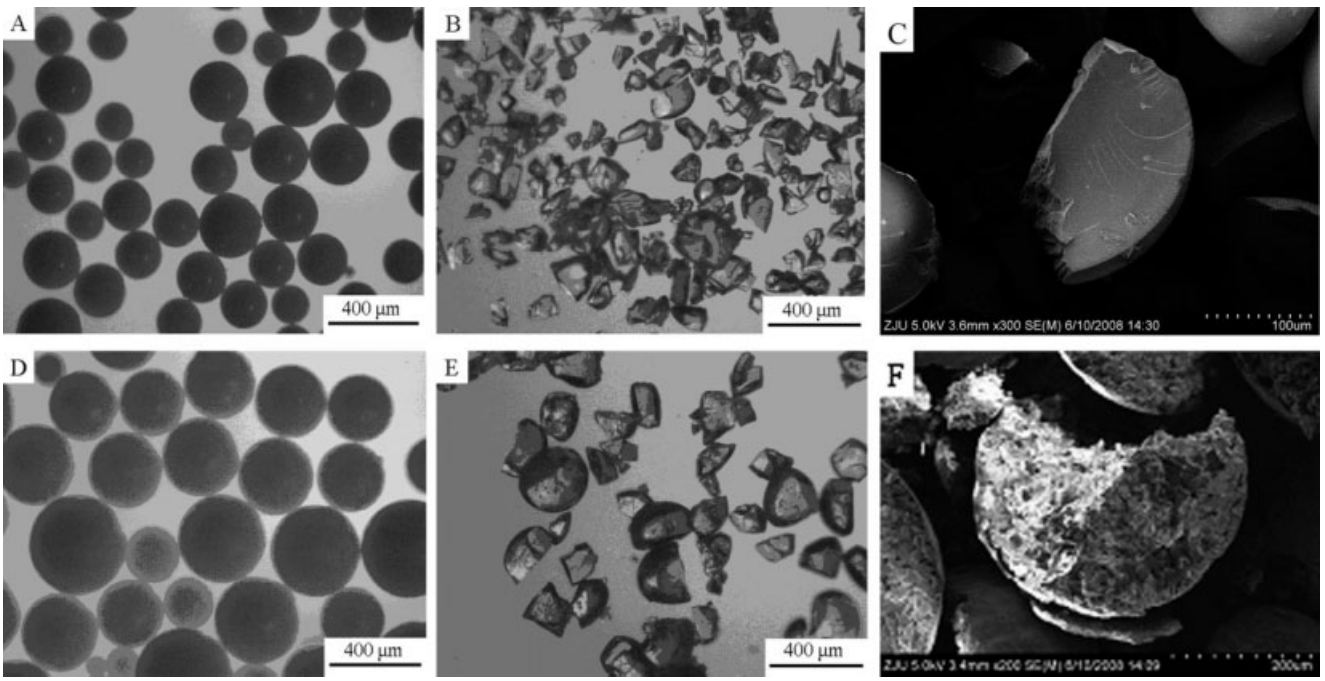

Figure 6 Typical microscope and SEM photos of the precursor microspheres and H-PS materials: (A) F02, (B,C) HF02, (D) F06, and (E,F) HF06.

wrapped by a poly (vinylbenzyl chloride) membrane. Then, in the second step, the precursors were swollen in DCE, and part of the outside noncrosslinked poly(vinylbenzyl chloride) layer dissolved in the solvent. At the same time, the VBC block was further crosslinked in the presence of the $FeCl_3$ as catalyst.

This mechanism was supported by the data of pore structure of the precursor microspheres and the partly nonspherical shape of the H-PS materials. On one hand, the internal morphology of the precursors derived from SEM proved that the inner part of the precursor microspheres had porosity; however, the porosity data were almost zero because the porous copolymer particles were wrapped in a nonporous poly(vinylbenzyl chloride) membrane. After the second step, the nonporous membrane was dissolved or further crosslinked; therefore, the porosity of the H-PS materials was available in the N_2 sorption and Hg intrusion measurements. On the other hand, the precursor samples observed under a microscope were strictly spherical, whereas the H-PS materials could hardly keep sphericity (Fig. 6), which convinced us that later formed PVBC polymer covered the copolymer particles and presented a spherical structure. Then, in the second step, because the outside PVBC was further crosslinked or partly dissolved in DCE, the spherical shape was broken. Moreover, a distinct membrane was observed in the SEM photo of HF06 [Fig. 6(F)], which further certified the previous mechanism and its schematic model.

CONCLUSIONS

H-PS materials with a bimodal pore size distribution and a controllable macroporosity were prepared via the combination of suspension polymerization and postcrosslinking. With various levels of PP in the coporogen, the effects of the PP weight fraction in toluene on SSA, the average pore size, the pore volume, the pore size distribution, and the solvent uptake data were investigated. The results indicate that the addition of a low level of PP porogen yielded higher SSA because of the improved pore connectivity. As the mass ratio of PP was further increased, the macroporosity of the H-PS materials progressively increased. This fact indicated that the aim of bimodal distribution and controllable macroporosity were achieved with PP in toluene as a coporogen. Finally, a possible mechanism of monomer polymerization and pore formation was proposed according to the experimental phenomena and results.

References

1. Davankov, V.; Pastukhov, A. V.; Tsyurupa, M. P. J Polym Sci Part B: Polym Phys 2000, 38, 1553.
2. Penner, N. A.; Nesterenko, P. N.; Ilyin, M. M.; Tsyurupa, M. R.; Davankov, V. A. Chromatographia 1999, 50, 611.
3. Jagodzinski, J. J.; Marshall, G. T.; Poulsen, B. J.; Raza, G.; Rolls, W. A. Chromatographia 1992, 591, 49.
4. Liu, Q. Q.; Wang, L.; Xiao, A. G. Des Monomers Polym 2007, 10, 405.
5. Sidorov, S. N.; Volkov, I. V.; Davankov, V. A.; Tsyurupa, M. P.; Valetsky, P. M.; Bronstein, L. M.; Karlinsey, R. J Am Chem Soc 2001, 123, 10502.

6. Bunchongturakarn, S.; Jongsomjit, B.; Praserthdam, P. Catal Commun 2008, 9, 789.
7. Bronstein, L. M.; Goerigk, G.; Kostylev, M.; Pink, M.; Khotina, I. A.; Valetsky, P. M.; Matveeva, V. G.; Sulman, E. M. J Phys Chem B 2004, 108, 18234.
8. Liu, Q. Q.; Wang, L.; Xiao, A. G.; Yu, H. J.; Tan, Q. H. Eur Polym J 2008, 44, 2516.
9. Liu, Q. Q.; Wang, L.; Xiao, A. G.; Yu, H. J.; Tan, Q. H.; Ding, J. H.; Ren, G. Q. J Phys Chem C 2008, 112, 13171.
10. Davankov, V. A.; Tsyurupa, M. P.; Rogozhin, S. V. J Polym Sci Polym Symp 1974, 47, 95.
11. Davankov, V. A.; Tsyurupa, M. P. React Polym 1990, 13, 27.
12. Davankov, V. A.; Tsyurupa, M. P.; Rogozhin, S. V. J Polym Sci Symp 1974, 47, 189.
13. Ahn, J. H.; Jang, J. E.; Oh, C. G.; Ihm, S. K.; Cortez, J.; Sherrington, D. C. Macromolecules 2006, 39, 627.
14. Brunauer, S.; Emmet, P. H.; Teller, E. J Am Chem Soc 1938, 60, 309.
15. Okay, O. Prog Polym Sci 2000, 25, 711.
16. Macintyre, F. S.; Sherrington, D. C. Macromolecules 2004, 37, 7628.